JOURNAL OF MATERIALS SCIENCE 31 (1996) 1857–1863

Easy glass formation in magnesium-based Mg–Ni–Nd alloys

Y. Li
Department of Physics, National University of Singapore, Singapore 119620
H.Y. LIU
Department of Mechanical and Manufacturing Engineering, Singapore Polytechnic, Singapore 139651
H. JONES
Department of Engineering Materials, University of Sheffield, Sheffield, UK

A number of magnesium-based alloys containing up to 20 at % Ni and 15 at % Nd were cast directly into a wedge shaped mould and also rapidly solidified by chill-block melt-spinning to produce ribbons between 30 and 100 μm in thickness. The formation of the amorphous state in the wedge and ribbons was confirmed by X-ray diffraction and differential scanning calorimetry. The measured tensile fracture strength and microhardness of these ribbons were found to be in the range 330–630 MPa and 190–250 kg mm^{-2}, respectively, which are significantly higher than for conventional magnesium alloys. Critical cooling rates for the glass formation of these alloys were obtained from wedge section thickness, Bridgman growth, thermal analysis data by differential thermal analysis and computational methods. The significance of several parameters for the glass-forming ability of these alloys is discussed.

1. Introduction

The recent discovery [1, 2] of high tensile strength amorphous aluminium and magnesium alloys has prompted renewed interest in such rapidly solidified light alloys. It was found [3–6] that the fully amorphous phase was formed in the Mg–Ni–X (X = La [3], Ce [4] and Y [5]), Mg–Cu–Y [5] and other magnesium-based systems [6] with combined alloy additions in the range 10–80 at %. The tensile fracture strength of the as-spun ribbons was in the range 535–850 MPa which is much higher than for conventional magnesium-based casting alloys [7].

More significantly, easy glass formation in diameters as large as 4 mm has been found in some metallic alloys, such as from the Mg–Cu–Y alloy system, by low-pressure chill-casting [8]. Such large dimensions for direct glass formation have not been obtained for conventional nickel- and iron-based metallic glass alloys, for which high cooling rates in the range 10^4–10^6 K s^{-1} were generally needed, and so the size of the sample in at least one dimension must be very small ($\leq$100 μm).

This paper presents results on glass formation, mechanical properties and thermal properties in alloys of the Mg–Ni–Nd system produced by wedge chill casting, Bridgman unidirectional solidification and melt-spinning. The critical cooling rates for glass formation were determined from the critical wedge section thickness, the critical velocity in unidirectional Bridgman growth, thermal analysis data by differential thermal analysis (DTA) and via computational methods. The glass-forming ability of these alloys is also discussed.

2. Experimental procedure

Eight magnesium-based Mg–Ni–Nd alloys (compositions in Table I) were made by induction melting 99.99% pure magnesium with combinations of 99.9% Nd, 99.9% Ni and Nd–33 wt % Ni master alloy in an argon atmosphere. The alloys were cast directly into a wedge-shaped copper mould having a wedge angle of 9°. Parts of these alloy wedges were then remelted for melt-spinning. Melt-spinning was done under argon, the chamber having been evacuated to less than 10^{-3} torr (1 torr = 133.322 Pa) before back-filling with argon. The quartz melt expulsion nozzle bore size was 0.7 mm and the copper wheel speed was 18 m s^{-1}. The ribbons produced were typically 1 mm wide and 30–100 μm thick. The amorphous state of the ribbons was confirmed by X-ray diffraction (XRD).

The glass transition temperature, T_g, crystallization temperature, T_x, and onset melting point, T_m, offset melting point, T_L, and onset solidification of these alloys, were obtained using either a Du Pont 2100 differential scanning calorimeter (DSC) or a Du Pont 9100 differential thermal analyser (DTA). The remelting and resolidification of these ribbons were carried out at a constant heating rate of 0.67 K s^{-1} and at different cooling rates from 0.17–0.42 K s^{-1},

0022–2461

TABLE I Compositions of alloys investigated

	Alloy							
	1	2	3	4	5	6	8	9
Ni (at %)	10.4	14.6	10.1	15.5	19.9	18.2	19.9	5.4
Nd (at %)	10.2	9.6	15.0	15.2	5.1	5.3	14.8	5.2

respectively. Typically, a 60 mg sample was used in standard aluminium or platinum pans and the temperature scanned over a range from room temperature to about 670 K at a uniform heating rate of 0.67 K s^{-1} for DSC.

The tensile strength of the ribbon specimens was measured by means of a uniaxial tensile testing machine operated at a strain rate of 8.3×10^{-4} s^{-1} with a gauge length of 20 mm. Scanning electron microscopy (SEM) was used to characterize the fracture surface and to measure fracture surface area. Microhardness measurements were performed using an Olympus Vickers Microhardness Tester and a 100 g load was used. All the reported microhardness values are the average of at least ten individual measurements.

3. Results and discussion

3.1. Glass formation

Eight Mg–Ni–Nd alloy wedges showed a sharp transition in surface appearance, and the X-ray diffraction (Fig. 1) and DSC results (Fig. 2a) confirmed the amorphous state at the thin end with a thickness as large as 3.5 mm for alloy 8 [9]. Fig. 2b shows the DSC traces recorded from melt-spun ribbons of these eight alloys and their amorphous state was confirmed. The characteristic glass transition temperature, T_g, and crystallization temperature, T_x, from these traces, together with critical thickness for glass formation, are given in Table II.

The results in Table II indicated that, with one exception, the critical thickness, z_{crit}, for glass formation by chill casting increases with increasing neodymium or nickel content for a fixed content of either alloy addition, over the composition studied. Fig. 3 shows a good correlation between $T_x - T_g$ and z_{crit} for the present series of alloys, i.e. the larger the value of $T_x - T_g$, the larger was z_{crit}. A similar correlation is implied by the results of Inoue *et al.* [8] for $Mg_{90-X}Cu_XY_{10}$ with $10 \leq X \leq 35$, though our alloy 8 required a $T_x - T_g$ of only 36–40 K to give a z_{crit} of 3.5 mm in a flat chill-cast wedge, whereas their easiest glass-forming composition, $Mg_{65}Cu_{25}Y_{10}$ (at %) required a value of 60 K to give a critical diameter of between 4 and 5 mm for glass formation in a chill-cast rod.

3.2. Mechanical properties of the ribbons

Measurements of tensile fracture strength, σ, Young's modulus, E, tensile fracture strain ε, and microhardness of the as-spun ribbons, are summarized in Table III. As seen in Table III, σ is in the range 330–625 MPa, while Young's modulus, E, and fracture strain, ε, lie in the range 30–51 GPa and 0.009–0.014, respectively. The tensile strengths are higher than the values of 200–300 MPa [7], typical of conventional magnesium-based casting alloys. Although the compositions and microhardness of the present alloys are similar to those reported by Inoue *et al.* [4, 5], the tensile fracture strength and Young's modulus of the present alloys are generally lower than those in the range 535–850 MPa reported [4, 5] for Mg–Ni–Ce, Mg–Cu–Y and Mg–Ni–Y ribbons as spun. The fracture strains, ε, are in the same range as

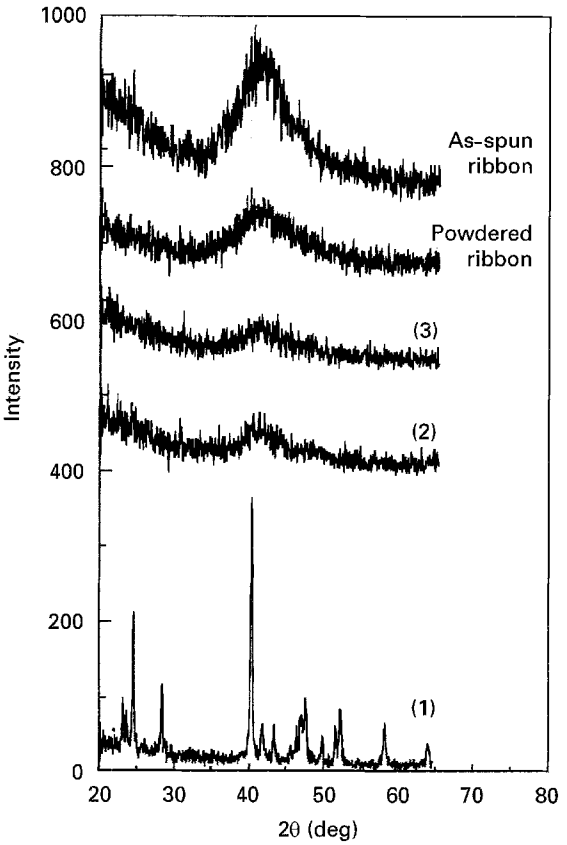

Figure 1 X-ray diffractograms from alloy 8 samples wedge chill-cast, where section thicknesses are (1) 6.2, (2) 3.0 and (3) 1 mm, respectively, compared with pulverized and as-spun chill block melt spun ribbon.

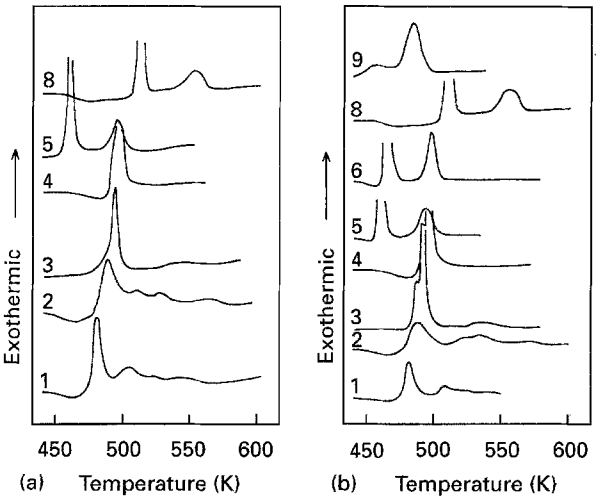

Figure 2 DSC traces for (a) glassy tips of chill-cast wedges, and (b) glassy melt-spun ribbons of the eight alloys studied. Heating rate 40 K min^{-1}.

TABLE II Results of DSC analysis of glassy samples from chill-cast wedges and melt-spun ribbons, together with critical thickness, z_{crit}, for glass formation in wedges

Alloy	Chill-cast					Melt-spun ribbon			
	Sample thickness (mm)	T_g (K)	T_x (K)	$T_x - T_g$ (K)	Critical thickness (mm)	Sample thickness (μm)	T_g (K)	T_x (K)	$T_x - T_g$ (K)
1	0.44	453	467	16	0.6	40–50	458	470	12
2	1.00	450	472	22	2.8	50–60	455	473	18
3	0.38	–	472	–	0.7	50–60	–	480	–
4	0.42	473	486	13	1.0	30–40	472	484	12
5	0.50	–	453	–	0.4	30–40	450	456	6
6	–	–	–	–	≤0.1	60–80	456	460	4
8	0.69	467	507	40	3.5	30	467	503	36
9	–	–	–	–	≤0.1	70–100	–	462	–

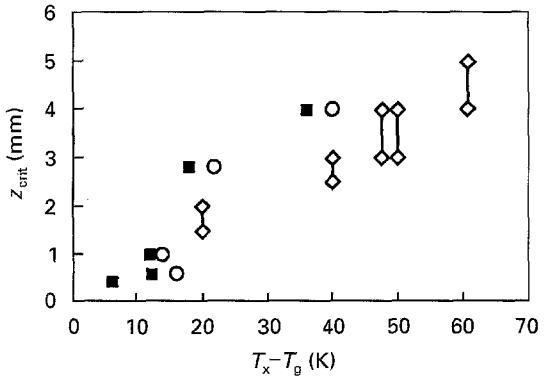

Figure 3 Critical thickness, z_{crit}, for glass formation by chill-casting as a function of difference $T_x - T_g$ between crystallization and glass transition temperatures for Mg–Ni–Nd (wedge chill-cast, present work, (○) $T_x - T_g$ measured for wedge cast material, (■) $T_x - T_g$ measured on melt-spun ribbon of same composition) and Mg–Cu–Y (chill-cast rods, Inoue *et al.* [8], ◇).

TABLE III Mechanical properties of Mg–Ni–Nd alloys as-spun

Alloy	σ (MPa)	E (GPa)	ε (σ/E)	Microhardness ($kg\,mm^{-2}$)
1	431	33	0.013	212 ± 6
2	483	41	0.012	234 ± 13
3	386	32	0.012	233 ± 5
4	625	51	0.012	231 ± 7
5	353	38	0.009	241 ± 14
6	434	47	0.009	247 ± 7
8	330	30	0.011	244 ± 10
9	375	39	0.011	197 ± 4

for Mg–Ni–Ce, but lower than those (0.014–0.018) reported for Mg–Cu–Y and Mg–Ni–Y ribbons. The alloy content of 30 at % at which the highest values of σ and E were obtained for $Mg_{70}Ni_{15}Nd_{15}$, is slightly higher than the 20–25 at % for the alloys reported by Inoue *et al.* [4, 5]. Values of microhardness H in Table III are typically within a few per cent of values expected from the relationship $H = 150 + 3.5X$ (where X is the total alloying content in at %) given by the results of Inoue *et al.* [8] for Mg–Ni–Y and Mg–Cu–Y glasses over the range $15 \leq X \leq 45$. All the samples were characteristically ductile in bending when they were made sufficiently thin.

3.3. Critical cooling rates for glass formation

The critical cooling rates for glass formation of these alloys were determined using several methods.

3.3.1. Wedge casting and Bridgman unidirectional solidification

The critical section thickness for glass formation by wedge casting for alloys 1, 4, 2 and 8 ($Mg_{80}Ni_{10}Nd_{10}$, $Mg_{70}Ni_{15}Nd_{15}$, $Mg_{75}Ni_{15}Nd_{10}$ and $Mg_{65}Ni_{20}Nd_{15}$) were 0.6, 1.5, 2.8 and 3.5 mm, respectively. Estimation of cooling rate as a function of section thickness of the wedge indicates that the corresponding cooling rates were about 200, 80 and 60 $K\,s^{-1}$ for alloys 2, 4 and 8, respectively, under their casting conditions.

Alloy 8 was also subjected to Bridgman unidirectional growth [10]. This involved remelting prior to steady withdrawal at constant pre-determined velocity in the range of 0.5–2.4 $mm\,s^{-1}$ through a temperature gradient of about 15 $K\,mm^{-1}$ into a water bath. Alloy 8, $Mg_{65}Ni_{20}Nd_{15}$ has an applicable critical cooling rate of 30 $K\,s^{-1}$ for glass formation during Bridgman growth, corresponding to the production of the critical front velocity of 2 $mm\,s^{-1}$ for glass formation at the applicable temperature gradient of 15 $K\,mm^{-1}$.

3.3.2. DTA

The critical cooling rate, R_C, for the formation of an amorphous phase can be evaluated from the relation [11–15]

$$\ln R = \ln R_C - \frac{b}{(T_L - T_{XC})^2} \quad (1)$$

where R is the cooling rate and b is a materials constant. T_L and T_{XC} are the offset temperature of fusion and the onset temperature of solidification, respectively. By measuring T_L upon melting at a constant heating rate and T_{XC} upon cooling at different cooling rates, R, using differential thermal analysis (DTA), the critical cooling rate for glass formation can be determined from the plot of $\ln(R)$ versus $1/(T_L - T_{XC})^2$.

Table IV lists the measured T_L and T_{XC} at cooling rates, R, ranging from 0.17–0.38 $K\,s^{-1}$ for alloys 1, 2,

TABLE IV Offset temperature of fusion, (T_L), and onset temperature of solidification, T_{XC}, as a function of cooling rate, and critical cooling rate, R_C, for glass formation in Mg–Ni–Nd alloys

$Mg_{80}Ni_{10}Nd_{10}$ $T_L = 780.8 \pm 0.4$ K		$Mg_{70}Ni_{15}Nd_{15}$ $T_L = 793.9 \pm 0.6$ K		$Mg_{75}Ni_{15}Nd_{10}$ $T_L = 779.7 \pm 0.4$ K		$Mg_{65}Ni_{20}Nd_{15}$ $T_L = 794.0 \pm 0.2$ K	
R (K s^{-1})	T_{XC} (K)	R (K s^{-1})	T_{XC} (K)	R (K s^{-1})	T_{XC} (K)	R (K s^{-1})	T_{XC} (K)
0.172 ± 0.002	722.2 ± 0.1	0.173 ± 0.002	722.0 ± 0.7	0.172 ± 0.002	720.8 ± 0.1	0.173	721 ± 0.3
0.256 ± 0.002	720.9 ± 0.6	0.257 ± 0.002	721.2 ± 0.1	0.252 ± 0.002	719.5 ± 0.3	0.260 ± 0.002	720.7 ± 0.1
0.36 ± 0.01	719.9 ± 0.6	0.375 ± 0.003	718.9 ± 0.2	0.383 ± 0.007	717.5 ± 0.4	0.38 ± 0.1	716.5 ± 0.3
$R_C = 3500 \pm 1200$ K s^{-1}		$R_C = 1400 \pm 700$ K s^{-1}		$R_C = 400 \pm 310$ K s^{-1}		$R_C = 50 \pm 20$ K s^{-1}	
$b = 34000 \pm 1200$ K^2		$b = 46000 \pm 13000$ K^2		$b = 27000 \pm 2000$ K^2		$b = 30000 \pm 15000$ K^2	

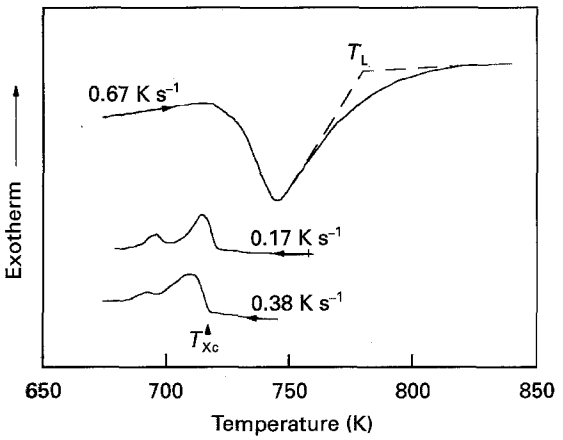

Figure 4 Differential thermal analysis (DTA) curves for alloy 2, $Mg_{75}Ni_{15}Nd_{10}$ [26].

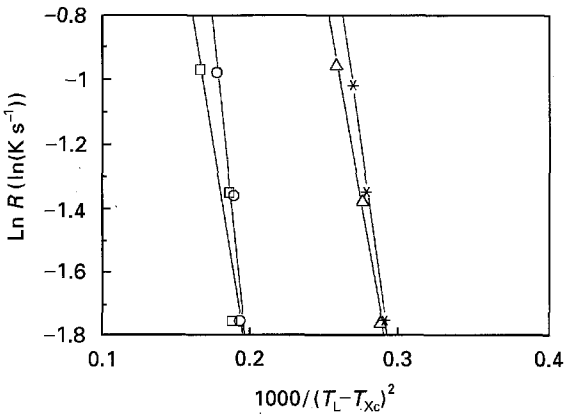

Figure 5 Plot of ln$R$ versus $1000/(T_L - T_{XC})^2$ for the four Mg–Ni–Nd alloys: (*) alloy 1, $Mg_{80}Ni_{10}Nd_{10}$; (○) alloy 4, $Mg_{70}Ni_{15}Nd_{15}$; (△) alloy 2, $Mg_{75}Ni_{15}Nd_{10}$; (□) alloy 8, $Mg_{65}Ni_{20}Nd_{15}$ [26].

4 and 8. Typical DTA curves (from alloy 2, $Mg_{75}Ni_{15}Nd_{10}$) exhibiting an endothermic peak upon melting and exothermic peaks upon solidification, are shown in Fig. 4. The offset melting temperature, T_L, for this alloy is 779.7 ± 0.4 K and the onset solidification temperature, T_{XC}, decreases from 720.8 ± 0.1 K to 717.5 ± 0.4 K with increase of cooling rate from 0.17 K s^{-1} to 0.38 K s^{-1}. The corresponding plot of ln(R) versus $1/(T_L - T_{XC})^2$ is shown in Fig. 5 and the resulting critical cooling rates obtained from Fig. 5 range from 3500 ± 1200 K s^{-1} for alloy 1 to 50 ± 20 K s^{-1} for alloy 8 (Table IV). The error mainly results from the limited accuracy of the temperature measurements T_L and T_{XC}.

3.3.3. Computational method

Based on accepted theories of nucleation, crystal growth and transformation kinetics, Uhlmann [16] has found that the time, t (s), for a given volume fraction, x, to crystallize is

$$t = \frac{9.32\eta}{kT}\left\{\frac{a_0^9 x \exp(1.024/T_r^3\Delta T_r^2)}{N_v^0 f^3[1-\exp(-\Delta H \Delta T_r/RT)]^3}\right\}^{1/4} \quad (2)$$

where η is the viscosity, k is Boltzmann's constant, T is the absolute temperature, a_0 is the average atomic diameter, N_v^0 is the number of atoms per unit volume, ΔH is the molar heat of fusion, f is the fraction of sites on the interface where atoms are preferentially added or removed, and $T_r = T/T_m$ and $\Delta T_r = (T_m - T)/T_m$ where T_m is the melting temperature. By plotting

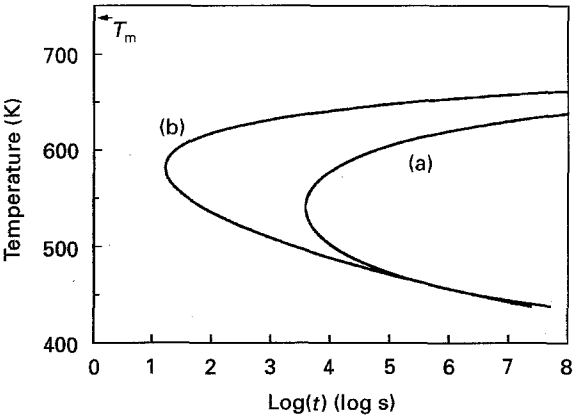

Figure 6 Computed time–temperature–transformation curves (a) and (b) using viscosities obtained from different estimations for $Mg_{65}Ni_{20}Nd_{15}$ [17].

T versus t, one can obtain the time–temperature–transformation (TTT) curve. The critical cooling rate, R_C (K s^{-1}), is defined as

$$R_C \approx (T_m - T_n)/t_n \quad (3)$$

where T_n and t_n are the temperature and time at the nose of the TTT curve, respectively.

The time–temperature–transformation curves were computed using Equation 2 and the relevant parameters [17]. Fig. 6 shows the computed TTT curves for alloy 8 ($Mg_{65}Ni_{20}Nd_{15}$) giving critical cooling rates for glass formation for this alloy of 0.015 ± 0.016 and 9.5 ± 3.4 K s^{-1}, respectively

(depending on the assumed temperature dependence of viscosity between alloy melting point, T_m, and glass transition temperature, T_g) [17].

The critical cooling rate for glass formation of 50 K s^{-1} for alloy 8 ($Mg_{65}Ni_{20}Nd_{15}$) obtained using DTA is in good agreement with the estimated cooling rate of 60 K s^{-1} obtained from the limiting wedge section thickness, but twice the value of 30 K s^{-1} obtained by using the Bridgman technique. The predicted critical cooling rates of 0.051 ± 0.016 and 9.5 ± 3.4 K s^{-1} are significantly lower than either 50 K s^{-1} evaluated from the DTA data or 60 and 30 K s^{-1} estimated from the wedge thickness and Bridgman growth measurements for the same alloy. The difference could be that the actual predicted values were calculated on the assumption that competitive crystallization from the melt is homogeneous, while the processes under the experimental conditions are almost certainly heterogeneous. This indicates that if the heterogeneous solidification were suppressed, the critical section thickness for glass formation of these Mg–Ni–Nd alloys could be increased dramatically.

A similar correlation between alloy content and critical cooling rates obtained using DTA and estimated from wedge section thickness was obtained. Evaluation of critical cooling rates for some lanthanum- and zirconium-based easy glass-forming alloys has been reported by Inoue *et al.* [14, 15] using the DTA and chill-casting method. The critical cooling rates determined for $La_{55}Al_{25}Ni_{20}$ [14], $Zr_{65}Al_{7.5}Ni_{10}Cu_{17.5}$ [15] were 87 and 1.5 K s^{-1}, respectively, using DTA methods. Fig. 7 shows a good correlation between the critical cooling rates and critical cooling section thickness or diameter for glass formation by chill casting in Mg–Ni–Nd [9], $Zr_{65}Al_{7.5}Ni_{10}Cu_{17.5}$ [15] and $La_{55}Al_{25}Ni_{20}$ [18] alloys. The temperature difference, ΔT, between the glass transition temperature, T_g, and crystallization temperature, T_x, is usually used to reflect the glass-forming ability [9, 19]. The corresponding plot of the critical cooling rate determined by DTA for $La_{55}Al_{25}Ni_{20}$, $Zr_{65}Al_{7.5}Ni_{10}Cu_{17.5}$ and the present alloys as a function of ΔT is shown in Fig. 7. The good correlation between the critical cooling rate, R_C, for glass formation evaluated by DTA and ΔT indicates that both R_C and ΔT can be used to reflect the glass-forming ability of these easy glass-forming alloys.

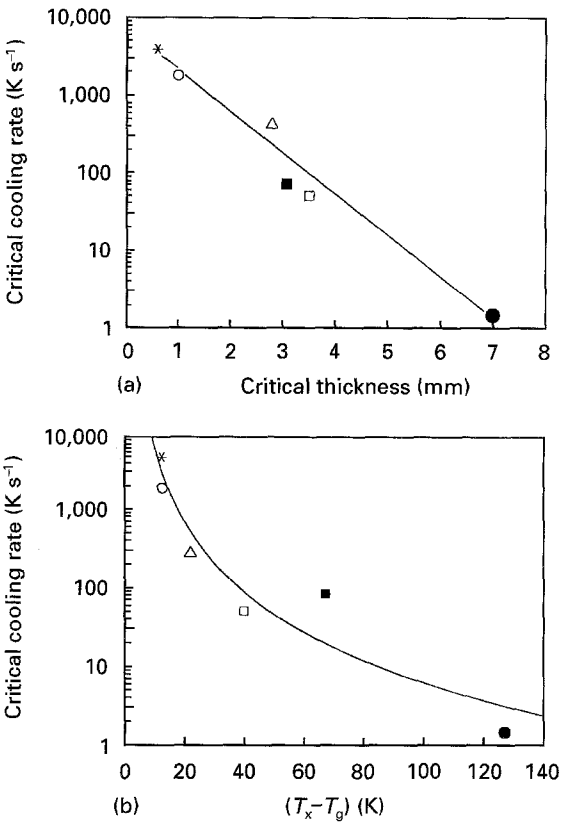

Figure 7 Correlation between the critical thickness and critical coling rates, and between $(T_x - T_g)$ and critical cooling rates. (a) Critical cooling rate for glass formation obtained by DTA as a function of critical thickness for glass formation in Mg–Ni–Nd (wedge chill-casting, present work, □), $Zr_{65}Al_{7.5}Ni_{10}Cu_{17.5}$ (Chill-cast rod, Inoue *et al.* [15, 25], ●), $La_{55}Al_{25}Ni_{20}$ (Inoue *et al.* [15, 25], ■). (b) Critical cooling rates for glass formation obtained by DTA as a function of the difference $(T_x - T_g)$ between crystallization and glass transition temperatures. The symbols are the same as in (a) [26].

3.4. Glass-forming ability

Several parameters have been used to reflect the glass-forming ability (GFA) in metallic alloys, particularly for those alloys based on nickel, iron and palladium in which rapid quenching from the melt at cooling rates in the range 10^4–10^6 K s^{-1} are needed to obtain glass formation in these alloys, and the sample thickness in one dimension must usually be very small (≤ 100 μm) [20–23]. The low critical cooling rate of 60 K s^{-1} and relatively large value of section thickness up to 3.5 mm for glass formation in Mg–Ni–Nd alloys thus indicates high GFA of these alloys. Thus it is of interest to determine the extent to which these established parameters predict easy glass formation in the present alloys.

One parameter used for GFA is the ratio between the glass transition temperature, T_g, and melting point, T_m, which was referred to as the reduced glass temperature, T_{rg} [20, 21]. Nickel, with an estimated T_{rg} of about 0.25 [24] and $Pd_{78}Cu_6Si_{16}$, with $T_{rg} = 0.66$ [24], represent close to opposite ends of the established range of T_{rg} for known metallic glasses. The characteristic glass transition temperature, T_g, crystallization temperature, T_x, and melting point, T_m, for the present alloys are given in Table V, together with the values for $Zr_{65}Al_{7.5}Ni_{10}Cu_{17.5}$ [25], $La_{55}Al_{25}Ni_{20}$ [4], and $Mg_{65}Cu_{25}Y_{10}$ [8] alloys which also showed high critical diameters for glass formation. As shown in Table V, the values of T_{rg} for these alloys are between 0.62 and 0.69, i.e. close to the high end of the T_{rg} range. However, these values do not reflect the differences in the glass-forming ability among these alloys themselves which have different critical thickness or diameters for glass formation, which do not correlate well with T_{rg}.

Donald and Davies [22] proposed that the GFA of alloys could be related to a parameter

$$\Delta T^* = \frac{T_m^{mix} - T_m}{T_m^{mix}} \quad (4)$$

TABLE V Results of DSC analysis of Mg–Ni–Nd as-spun ribbons, together with parameters for GFA and critical section diameter for glass formation of easy glass-forming compositions based on magnesium, lanthanum and zirconium

Alloy	T_g (K)	T_x (K)	T_m (K)	T_{rg}	ΔT^*	ΔT	K	Critical section thickness or diameter (mm)
1	458	470	719	0.65	0.35	12	0.039	0.6
2	455	473	719	0.66	0.37	18	0.058	2.8
3	–	480	741	0.65	–	0	0	–
4	472	484	728	0.66	0.38	12	0.039	1.0
5	450	456	712	0.64	0.41	6	0.012	–
6	456	460	717	0.64	0.41	4	0.014	–
8	467	503	738	0.68	0.41	36	0.127	3.5
9	–	462	742	0.62	0.27	0	0	–
$Zr_{65}Al_{7.5}Ni_{10}Cu_{17.5}$ [25]	622	749	1072	0.61	0.32	127	0.39	7.0
$La_{55}Al_{25}Ni_{20}$ [4]	487	545	707	0.69	0.27	58	0.36	3.0
$Mg_{65}Cu_{25}Y_{10}$ [8]	425	486	713	0.60	0.26	61	0.27	4.0

which represents the fractional departure of T_m from the simple rule of mixtures for melting temperature, T_m^{mix}, where

$$T_m^{mix} = \sum^{n} x_i T_m^i \quad (5)$$

and x_i and T_m^i are the mole fraction and melting point, respectively, of the ith component of an n-component alloy. It was found [22] that most of the glass-forming alloys, such as iron- and nickel-based metallic glasses, had values of $\Delta T^* \geq 0.2$. The ΔT^* values listed in Table V for the present alloys are larger than 0.2. The values, however, are similar to each other so again this criterion failed to pin-point which of these alloys has the highest GFA.

The temperature span, ΔT, between the glass transition temperature, T_g, and crystallization temperature, T_x, was also regarded as an empirical indicator of glass-forming ability. Generally, the larger the temperature interval, ΔT, the higher is the GFA. A good correlation exists between ΔT and critical thickness, z_{crit}, for glass formation by chill-casting for the present alloys, as shown in Fig. 3. A similar correlation was implied by the results of Inoue *et al.* [14] for $Mg_{90-X}Cu_XY_{10}$ with $10 \leq X \leq 35$. These results indicate that the temperature interval ΔT is a good indicator of GFA for these easy glass-forming alloys.

Hruby also suggested [23] that GFA can be correlated with a parameter, K

$$K = \frac{T_x - T_g}{T_m - T_x} \quad (6)$$

It can be seen from Table V that the larger the K, the larger is the critical thickness or diameter, indicating that the parameter K does correlate with glass-forming ability for these easy glass-forming alloys. Fig. 8 shows that the correlation between the critical thickness or diameter with all the parameters of T_{rg}, ΔT^*, ΔT and K. The above calculation shows that there is no apparent correlation between critical section thickness or diameter, d_{crit}, and parameters T_{rg} and ΔT^*, indicating that these two parameters have failed to represent relative GFA among these easy glass-forming systems. There are, however, correlations between

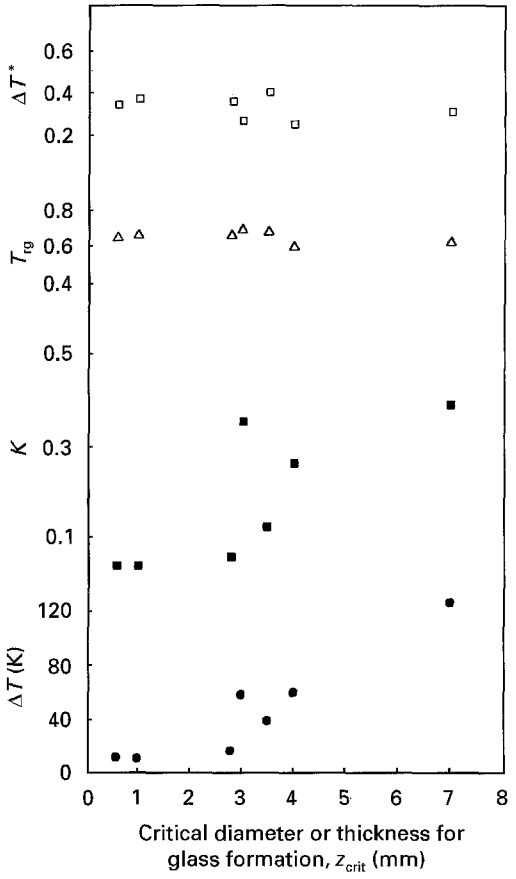

Figure 8 The parameters used to show GFA as a function of critical section thickness or diameter for glass formation. Data from Table V.

critical section thickness or diameters, d_{crit}, and parameters ΔT and K, indicating that these two parameters can be used to identify easy glass formation in these systems.

4. Conclusions

1. Easy glass formation has been found in a number of magnesium-based alloys containing up to 20 at % Ni and 15 at % Nd under wedge chill-casting with critical section thickness as large as 3.5 mm or melt-spinning conditions.

2. Tensile strength, σ, Young's modulus, E, and microhardness in the range 330–630 MPa, 30–51 GPa and 190–250 kg mm^{-2}, respectively, were obtained for glassy Mg–Ni–Nd melt-spun ribbons for the composition range up to 20 at % Ni and 15 at % Nd.

3. The critical cooling rates for glass formation of Mg–Ni–Nd were also evaluated by using DTA and they correlate well with those from the critical section thickness.

4. The predicted critical cooling rate for $Mg_{65}Ni_{20}Nd_{15}$ using the kinetic theory of crystallization based on standard theories of homogeneous nucleation and crystallization, were found to be lower than the experimental values, indicating that if heterogeneous nucleation was suppressed, a much higher critical thickness for glass formation could be obtained for this alloy.

5. There is no apparent correlation between critical section thickness or diameter, z_{crit}, and parameters T_{rg} and ΔT^*, indicating that these do not rank GFA effectively among these easy glass-forming systems. There are, however, correlations between z_{crit} and parameters ΔT and K indicating that these two can be used to represent relative GFA for easy glass-forming systems.

Acknowledgements

The wedge casting and melt-spinning of the magnesium alloys and partial thermal analysis were carried out at the University of Sheffield, and the rest of the experiments, including mechanical testing of the ribbons and the computation, were carried out at the National University of Singapore.

References

1. Y. H. KIM, A. INOUE and T. MASUMOTO, *Mater. Trans. JIM* **31** (1990) 747.
2. A. INOUE, A. KATO, T. ZHANG, S.G. KIM and T. MASUMOTO, *ibid.* **32** (1991) 277.
3. A. INOUE, M. KOLINATA, A. TSAI and T. MASUMOTO, *ibid.* **30** (1989) 378.
4. A. INOUE, K. OHTERA, K. KITO, and T. MASUMOTO, *Jpn. J. Appl. Phys.* **127** (1988) L2248.
5. S. G. KIM, A. INOUE, and T. MASUMOTO, *Mater. Trans. JIM* **31** (1990) 929.
6. T. MASUMOTO and A. INOUE, US Pat. 4990 198 (1991).
7. "ASM Handbook", Vol. 2 (ASM International Society, Materials Park, OH, 1990) p. 455.
8. A. INOUE, A. KATO, T. ZHANG, S. G. KIM and T. MASUMOTO, *Mater. Trans. JIM* **32** (1991) 609.
9. Y. LI, H. JONES and H.A. DAVIES, *Scripta Metall. Mater* **26** (1992) 1371.
10. Y. LI, H. Y. LIU, H. A. DAVIES and H. JONES, *Mater. Sci. Eng.* **A179/A180** (1994) 628.
11. J. M. BARANDIARAN and J. COLMENERO, *J. Non-Cryst. Solids* **46** (1981) 277.
12. T. KANAMORI and S. TAKAHASHI, *Jpn. J. Appl. Phys.* **24** (1985) L758.
13. M. POULAIN, *J. Non-Cryst. Solids* **140** (1992) 1.
14. A. INOUE, T. ZHANG and T. MASUMOTO, *ibid.* **156–158** (1993) 473.
15. A. INOUE, T. ZHANG, N. NISHIYAMA, K. OHBA and T. MASUMOTO, *Mater. Trans. JIM* **34** (1993) 1234.
16. D. R. UHLMANN, *J. Non-Cryst. Solids* **7** (1972) 337.
17. Y. LI, *ibid.* **175** (1994) 224.
18. A. INOUE, T. ZHANG, and T. MASUMOTO, *Mater. Trans. JIM* **31** (1990) 425.
19. Y. LI, S. C. NG, C. K. ONG and H. JONES, *J. Mater. Processing Technol.* **48** (1995) 489.
20. D. TURNBULL, *Contemp. Phys.* **10** (1969) 473.
21. H. A. DAVIES and B. G. LEWIS, *Scripta Metall. Mater.* **9** (1975) 1109.
22. I. W. DONALD and H. A. DAVIES, *J. Non-Cryst. Solids* **30** (1978) 77.
23. A. HRUBY, *Czech. J. Phys.* **B22** (1972) 1187.
24. H. A. DAVIES, in "Proceedings of the 3rd International Conference on Rapidly Quenched Metals", edited by B. Cantor (Metals Society, London, 1978) p. 1.
25. T. ZHANG, A. INOUE and T. MASUMOTO, *Mater. Trans. JIM* **32** (1991) 1005.
26. Y. LI, S. C. NG, C. K. ONG, H. H. HNG and H. JONES, *J. Mater. Sci. Lett.* **14** (1995) 988.

Received 14 June
and accepted 7 November 1995